

Electronic Supplementary Information for

**Surface functionalization of discrete metal-chalcogenide
supertetrahedral clusters and the photocatalytic application**

Jin Wu^{a,b}, Qiang Fu,^b Zixin Wu,^b Peipei Sun,^{a,b} Xing Zhu,^c Ying Wang,^c Ning Chen,^b Dong-Sheng Li,^d and Tao Wu^{a,b,*}

^a *College of Chemistry and Materials Science, Guangdong Provincial Key Laboratory of Functional Supramolecular Coordination Materials and Applications, Jinan University, Guangzhou, Guangdong 510632, China.*

^b *College of Chemistry, Chemical Engineering and Materials Science, Soochow University, Suzhou, Jiangsu 215123, China.*

^c *Testing and Analysis centre, Soochow University, Suzhou, Jiangsu 215123, China.*

^d *College of Materials and Chemical Engineering, Hubei Provincial Collaborative Innovation Centre for New Energy Microgrid, Key Laboratory of Inorganic Nonmetallic Crystalline and Energy Conversion Materials, China Three Gorges University, Yichang 443002, China.*

*Corresponding author E-mail: wutao@jnu.edu.cn

Supplementary information

Characterizations:

Photoelectric Response. First, 5.0 mg of **ISC-24-ZnSnS**, **ISC-25-ZnSnS-SPh**, and **ISC-25-4'-NH₂**, and their corresponding composites powder (decorated MXenes, denoted as **CM_n**, while *n* represents the weight percentage of Ti₃C₂T_x nanosheets to the whole nanocomposites) was added to 10 mL of isopropanol with the presence of 1.5 mg of Mg(NO₃)₂·6H₂O (addition Mg(NO₃)₂·6H₂O for increasing conductivity), respectively. The mixture was then stirred for 1 h. The dispersed samples were electrodeposited onto cathodic indium-tin-oxide (ITO) conductive glass with a Pt plate electrode as the anode. The whole electrodeposition process lasted for 30 min under a constant working voltage of 30.0 V. The photocurrent experiment was carried out in a three-electrode electrochemical cell on a CHI760E electrochemical workstation. The sample-coated ITO glass (6 cm², effective area about 1 cm²) was used as the working electrode, the Pt line as the auxiliary electrode, and the saturated calomel electrode (SCE) as the reference electrode. The light source was a 150 W high-voltage xenon lamp located 20 cm from the surface of the ITO electrode. An aqueous solution of anhydrous sodium sulfate (0.5 M, 100 mL) was used as a supporting electrolyte.

Electrochemical impedance spectroscopy and Mott-Schottky analysis. The sample was plated on ITO glass as described above to make a working electrode. A three-electrode system was used for the test, with a platinum electrode as the auxiliary electrode and a glycerine electrode as the reference electrode. Electrochemical impedance testing was carried out using a 0.5 M Na₂SO₄ solution as the electrolyte solution, with a starting voltage setting of -0.05 V (vs RHE), a sine voltage setting of 5 mV and a scan range of 1 – 100 kHz.

Photocatalytic performance test. The photocatalytic hydrogen production (PHE) performance of the **P1-CNPs** and **CM_n** series samples were analyzed by in a closed gas circulation system. Sample preparation: 10 mg of **P1-CNPs** or **CM_n** series samples were dispersed in 90 mL of deionized water and 10 mL of 0.1M Na₂S/Na₂SO₃ was added as sacrificial reagent. The mixture was added to a quartz reactor and the system was fixed and vacuum pumped to ~1.0 kPa. Magnetic stirring of the mixture was maintained while a xenon lamp (300 W, PSL-SXE 300C, Perfect Light) with a wavelength of 320-780 nm was placed approximately 10 cm above the quartz reactor and irradiated at a controlled intensity of 168 mW·cm⁻². During the photocatalytic experiments, the temperature of the reaction solution was controlled at 5 °C using a recirculating cooling water system to prevent the mixed solution

from warming up due to prolonged irradiation and thus affecting the performance of the PHE. Product analysis was performed on a gas chromatograph (GC 7890 T, Shanghai, China) equipped with a thermal conductivity detector (TCD) and a 5 Å molecular sieve column, using N₂ as the carrier gas, and each photocatalytic experiment lasted 20 h. The sampling time was set at 1 h/time. The photocatalytic hydrogen production cycle for **P1-CNPs** and **CMn** series samples was performed as described above, and after the first run, the suspension was re-evacuated to 1.0 kPa and the photocatalytic hydrogen production experiment was continued, and the process was repeated three times.

Elemental Analysis. Energy dispersive spectroscopy (EDS) analysis was performed on scanning electron microscope (SEM) equipped with energy dispersive spectroscopy (EDS) detector. An accelerating voltage of 25 kV and 40 s accumulation time were applied. Elemental analysis of C, H, and N was performed on VARIDEL III elemental analyzer.

¹H-NMR Characterization. ¹H-NMR spectra were performed on an Agilent instrument (600 MHz) and internally referenced to the signals of tetramethylsilane. The crystals were washed by ethanol three times, dried and grounded before NMR testing. And the deuterated reagent used here was *d*⁶-DMSO.

UV-Vis Absorption. Room-temperature solid-state UV-Vis diffusion reflectance spectra of **ISC-24~26** and **CMn** series samples were measured on a SHIMADZU UV-3600 UV-Vis-NIR spectrophotometer coupled with an integrating sphere by using BaSO₄ powder as the reflectance reference. The absorption spectra were calculated from reflectance spectra by using the Kubelka-Munk function: $F(R)=\alpha/S=(1-R)^2/2R$, where R , α , and S are the reflection, the absorption and the scattering coefficient, respectively. In order to determine the band edge of the direct-gap semiconductor, the relation between the absorption coefficients (α) and the incident photon energy ($h\nu$) is exhibited as $\alpha h\nu = A(h\nu - E_g)^{1/2}$, where A is a constant that relates to the effective masses associated with the valence and conduction bands, and E_g is the optical transition gap of the solid material. The band gap of the obtained samples can be determined from the Tauc plot with $[F(R)*h\nu]^2$ vs. $h\nu$ by extrapolating the linear region to the abscissa.

Powder X-ray diffraction (PXRD). PXRD data were collected on a desktop diffractometer (D2 PHASER, Bruker, Germany) using Cu-K α ($\lambda = 1.54056$ Å) radiation operated at 30 kV and 10 mA.

Photoluminescence and Photoluminescence Excitation Spectra. Photoluminescence (PL) and photoluminescence excitation (PLE) spectra were recorded by a HORIBA scientific

Fluorolog-3 steady state and time-resolved fluorescence spectrophotometer equipped with a 450 W Xenon lamp. Low temperature PL spectra were recorded on a HORIBA scientific Fluorolog-3 spectrophotometer with a low temperature accessory.

Atomic Force Microscopy test. Atomic Force Microscopy tests on ultra-thin $\text{Ti}_3\text{C}_2\text{T}_x$ nanosheets were carried out with a Bruker ICON scanning probe microscope in Tapping mode. Sample preparation: The ultrasonically treated $\text{Ti}_3\text{C}_2\text{T}_x$ nanosheets were dispersed in deionized water, diluted with 9 times the volume of ethanol and then a small amount of the top layer was pipetted onto the surface of the ultra-clean silicon wafers, dried under vacuum and used for testing.

TEM, HRTEM, HAADF-STEM, and SAED characterizations. Transmission electron microscopy (TEM) and high-resolution transmission electron microscopy (HRTEM) images were taken by HT7700 (Hitachi, Japan) and FEI Tacnai G2 F20 (FEI, USA) equipment to determine the microstructure and morphology of **P1-CNPs** and **CM n** series composites. High-angle annular dark field-scanning transmission electron microscopy (HAADF-STEM) and selected area electron diffraction (SAED) images were taken by Talos F200X G2 (Thermo Scientific, Czech) to determine the microscopic morphology and elemental distribution of $\text{Ti}_3\text{C}_2\text{T}_x$ nanosheets and **CM1**.

Single-crystal X-ray diffraction characterization. The SCXRD measurements on **ISC-24**, **ISC-25** and **ISC-26** series samples were performed on a Bruker Smart CPAD area diffractometer with a nitrogen-flow temperature controller using graphite-monochromated $\text{MoK}\alpha$ ($\lambda = 0.71073 \text{ \AA}$) radiation at 120 K. The structures were solved by direct methods using SHELXS-2014 and the refinement against all reflections of the compounds was performed using SHELXL-2014.¹⁻³ In these structures, some cations and free solvent molecules were highly disordered and could not be located. The diffuse electron densities resulting from these residual cations and solvent molecules were removed from the data set using the SQUEEZE⁴ routine of PLATON and refined further using the data generated. The number of SQUEEZED electrons and their signature can be found in our cif files (CCDC 2254140-2254148). The general crystal data and refinement parameters of the **ISC-24**, **ISC-25** and **ISC-26** series samples are summarized and presented in Table S1.

X-ray photoelectron spectroscopy. X-ray photoelectron spectroscopy (XPS, Thermo Fisher Scientific ESCLAB 250Xi) was used to analyze the band structure of **CM n** series samples.

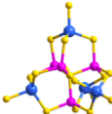
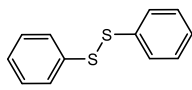
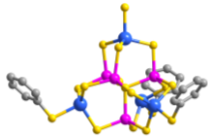
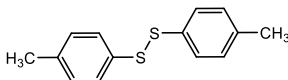
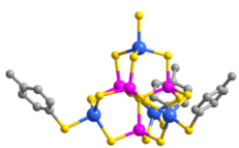
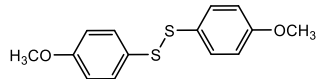
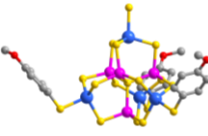
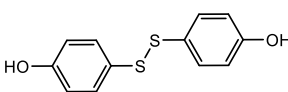
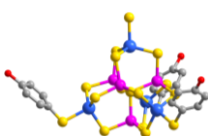
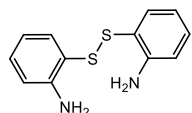
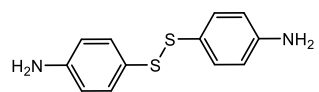
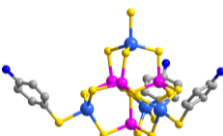
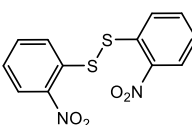
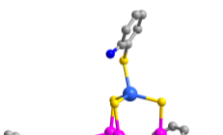
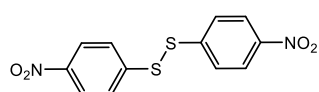
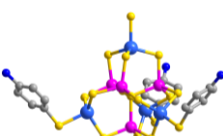
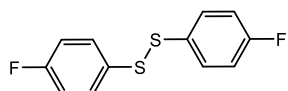
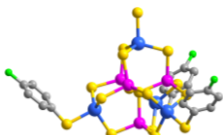
Table S1. The structural refinement parameters on series of **ISC-24**, **ISC-25**, and **ISC-26** compounds.

Compound	ISC-24-ZnSnS	ISC-25-ZnSnS-SPh	ISC-25-4'-NH ₂
Empirical formula	C ₆₃ N ₉ S ₁₇ Sn ₄ Zn ₄	C ₆₀ H ₁₁₁ N ₆ S ₁₇ Sn ₄ Zn ₄	C ₆₀ H ₁₀₈ N ₉ S ₁₇ Sn ₄ Zn ₄
Formula weight	2164.00	2197.82	2236.83
Morphology	Block	Rhombohedral	Rhombohedral
Crystal system	Cubic	trigonal	trigonal
Space group	<i>P</i> -43 <i>n</i>	<i>R</i> -3	<i>R</i> -3
<i>Z</i>	8	6	6
<i>T</i> /K	123.0	120.00	120.03
$\lambda/\text{\AA}$	0.71073	0.71073	0.71073
<i>a</i> /\AA	27.9828(7)	16.1766(5)	16.1920(5)
<i>b</i> /\AA	27.9828(7)	16.1766(5)	16.1920(5)
<i>c</i> /\AA	27.9828(7)	62.4763(18)	63.402(2)
α°	90	90	90
β°	90	90	90
γ°	90	120	120
<i>V</i> /\AA ³	21911.6(16)	14158.6(10)	14395.8(10)
<i>D</i> (g/cm ³)	1.312	1.547	1.548
μ/mm^{-1}	2.111	2.449	2.411
<i>F</i> (000)	8264.0	6630.0	6738.0
Col. refs.	197603	24122	16231
Indep. refs.	6218	5775	5791
GOF on <i>F</i> ²	1.194	1.064	1.022
<i>R</i> ₁ , <i>wR</i> ₂ (<i>I</i> > 2 σ (<i>I</i>))	0.0484 0.1237	0.0443 0.1145	0.0405 0.1010
<i>R</i> ₁ , <i>wR</i> ₂ (all data)	0.0588 0.1403	0.0565 0.1276	0.0524 0.1104

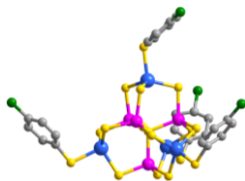
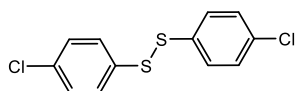
Compound	ISC-25-4'-CH ₃	ISC-25-4'-OCH ₃	ISC-25-4'-OH
Empirical formula	C ₆₄ N ₆ S ₁₆ Sn ₄ Zn ₄	C ₆₃ H ₁₁₇ N ₆ O ₃ S ₁₇ Sn ₄ Zn ₄	C ₆₀ H ₁₁₁ N ₆ O ₃ S ₁₇ Sn ₄ Zn ₄
Formula weight	2101.92	2287.90	2243.61
Morphology	Rhombohedral	Rhombohedral	Rhombohedral
Crystal system	trigonal	trigonal	trigonal
Space group	<i>R</i> -3	<i>R</i> -3	<i>R</i> -3
<i>Z</i>	6	6	6
<i>T</i> / <i>K</i>	119.97	120.03	120.01
$\lambda/\text{\AA}$	0.71073	0.71073	0.71073
<i>a</i> / \AA	16.2154(3)	16.1193(8)	16.2345(4)
<i>b</i> / \AA	16.2154(3)	16.1193(8)	16.2345(4)
<i>c</i> / \AA	63.6173(12)	64.468(4)	62.9138(17)
α°	90	90	90
β°	90	90	90
γ°	120	120	120
<i>V</i> / \AA^3	14486.4(6)	14506.6(17)	14360.0(8)
<i>D</i> (g/cm ³)	1.446	1.571	1.557
μ/mm^{-1}	2.371	2.396	2.420
<i>F</i> (000)	6012.0	6918.0	6767.0
Col. refs.	22034	40719	35647
Indep. refs.	5456	5895	5441
GOF on <i>F</i> ²	1.029	1.133	1.053
<i>R</i> ₁ , <i>wR</i> ₂ (<i>I</i> > 2 σ (<i>I</i>))	0.0464 0.1264	0.0388 0.0970	0.0426 0.1058
<i>R</i> ₁ , <i>wR</i> ₂ (all data)	0.0520 0.1322	0.0490 0.1056	0.0526 0.1165

Compound	ISC-25-4'-F	ISC-26-2'-NH ₂	ISC-26-4'-Cl
Empirical formula	C ₆₀ H ₁₀₈ F ₃ N ₆ S ₁₇ Sn ₄ Zn ₄	C ₇₀ N ₁₁ S ₁₇ Sn ₄ Zn ₄	C ₆₆ H ₁₁₂ Cl ₄ N ₆ S ₁₇ Sn ₄ Zn ₄
Formula weight	2252.99	2266.08	2412.67
Morphology	Rhombohedral	Rhombohedral	Rhombohedral
Crystal system	trigonal	trigonal	trigonal
Space group	<i>R</i> -3	<i>R</i> -3	<i>R</i> -3
<i>Z</i>	6	6	6
<i>T</i> /K	120.01	119.99	120.01
$\lambda/\text{\AA}$	0.71073	0.71073	0.71073
<i>a</i> /\AA	16.2345(3)	16.2406(5)	27.7207(6)
<i>b</i> /\AA	16.2345(3)	16.2406(5)	16.1476(3)
<i>c</i> /\AA	62.9138(17)	60.7220(18)	48.2286(12)
α°	90	90	90
β°	90	90	101.9120(10)
γ°	120	120	90
<i>V</i> /\AA ³	14360.0(7)	13870.1(9)	21123.3(8)
<i>D</i> (g/cm ³)	1.563	1.628	1.517
μ/mm^{-1}	2.424	2.506	2.294
<i>F</i> (000)	6777.0	6504.0	9680.0
Col. refs.	37284	40411	203282
Indep. refs.	5848	5635	17927
GOF on <i>F</i> ²	1.062	1.054	1.110
<i>R</i> ₁ , <i>wR</i> ₂ (<i>I</i> > 2σ(<i>I</i>))	0.0450 0.1168	0.0387 0.1101	0.0545 0.1300
<i>R</i> ₁ , <i>wR</i> ₂ (all data)	0.0568 0.1300	0.0436 0.1156	0.0649 0.1384

Table S2. Category of substitutes used in the synthetic processes.

Reactant formula	Reactant structure	Molecular structure of product cluster	Product abbreviation
/	/		ISC-24
(PhS) ₂			ISC-25
(CH ₃ PhS) ₂			ISC-25-4'-CH ₃
(CH ₃ OPhS) ₂			ISC-25-4'-OCH ₃
(HOPhS) ₂			ISC-25-4'-OH
(H ₂ NPhS) ₂		/	/
(H ₂ NPhS) ₂			ISC-25-4'-NH ₂
(O ₂ NPhS) ₂			ISC-26-2'-NH ₂
(O ₂ NPhS) ₂			ISC-25-4'-NH ₂
(FPhS) ₂			ISC-25-4'-F

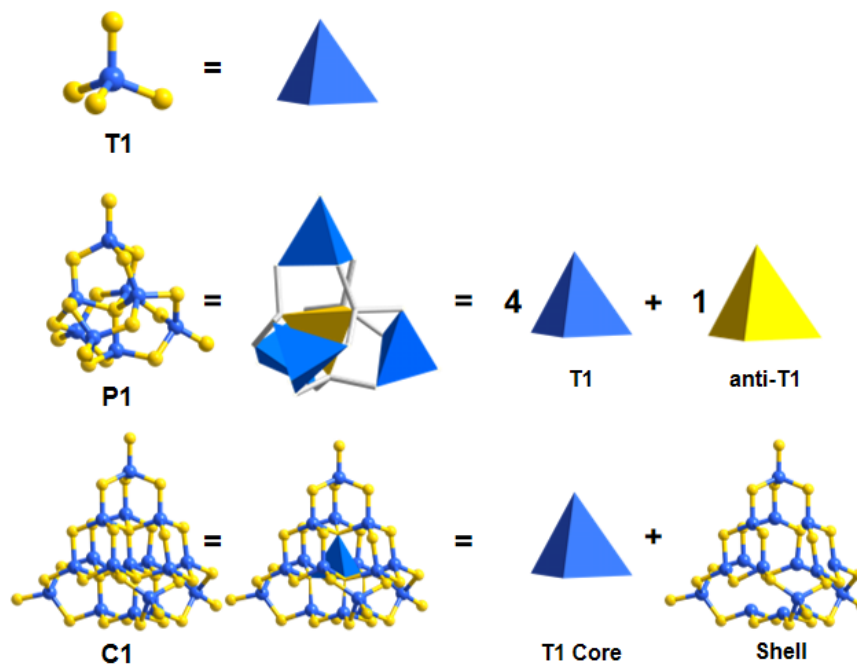
(ClPhS)₂



ISC-26-4'-Cl

Table S3. Elemental analysis of C, H, and N components for ISC-24, ISC-25, and ISC-25-4'-NH₂.

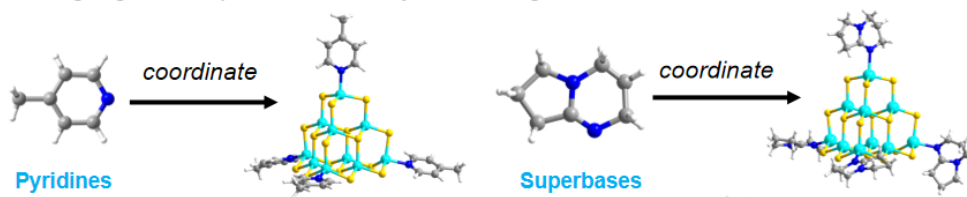
Elements (wt%)		C (%)	H (%)	N (%)
ISC-24	Calculated	34.68	6.65	5.77
	Experimental	34.32	6.28	5.42
ISC-25	Calculated	34.80	5.53	4.24
	Experimental	34.44	5.51	4.01
ISC-25-4'-NH ₂	Calculated	34.13	5.55	5.94
	Experimental	34.06	5.46	5.81



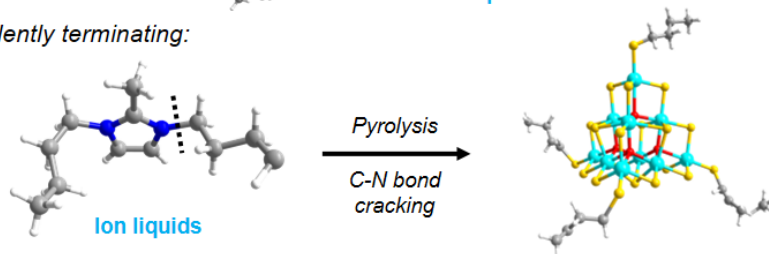
Scheme S1. Molecular structure of the main structural types of MCSCs. T_n is the simplest unit, P_n and C_n are developed from the corresponding T_n structure, where n represents the number of metal layers in the basic cluster units.

Synthetic Methods for Partially-Protected MCSCs:

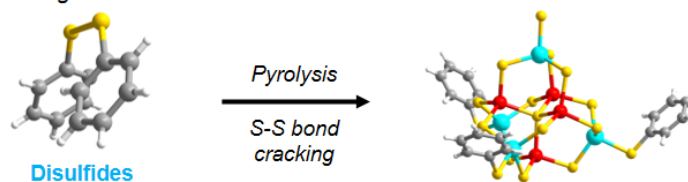
(a) *N*-containing organic template coordinately terminating:



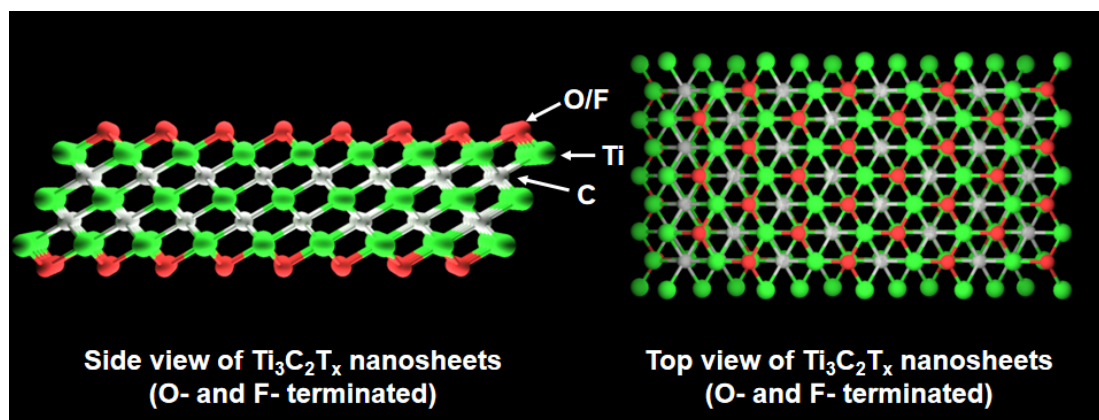
(b) Alkyl covalently terminating:



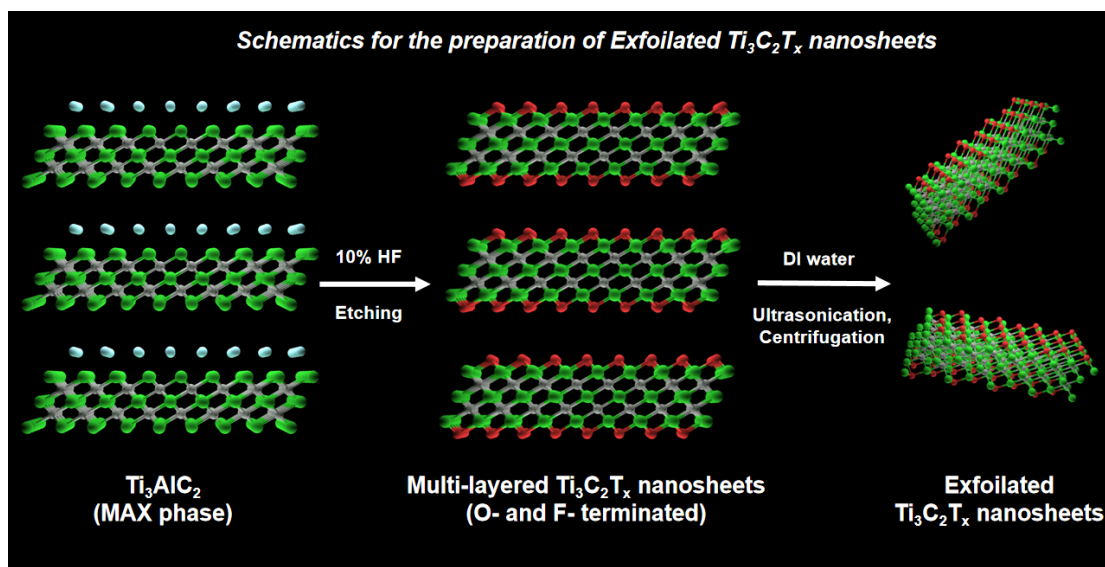
(c) Aryl covalently terminating:



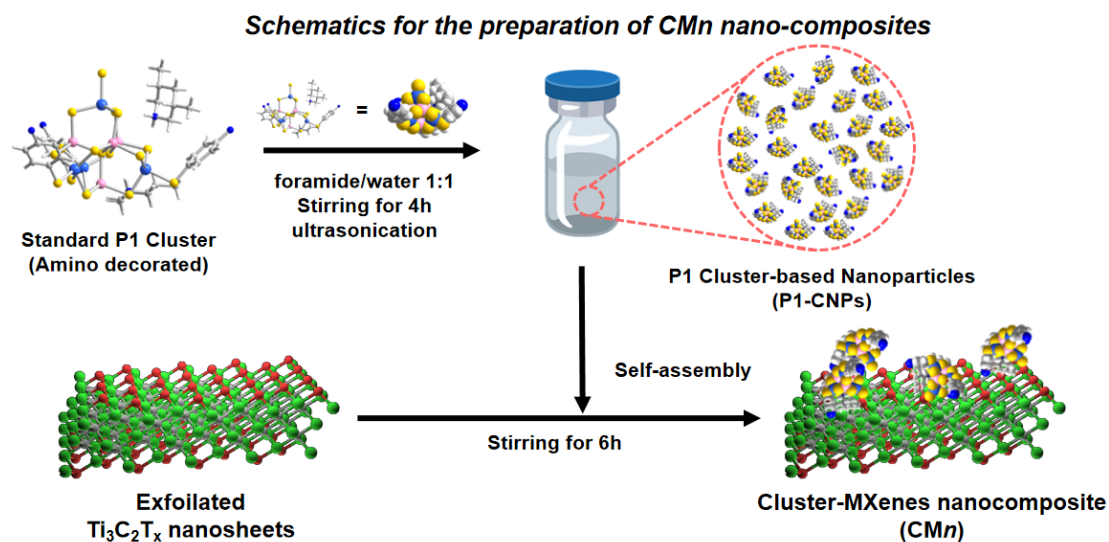
Scheme. S2. Summary of the synthetic methods for the existing partially-protected MCSCs.



Scheme. S3. Structure of $\text{Ti}_3\text{C}_2\text{T}_x$ nanosheets.



Scheme. S4. Schematic charts for the synthetic procedure of $Ti_3C_2T_x$ nanosheets.



Scheme. S5. Schematic charts for the fabrication process of CM_n nanocomposites.

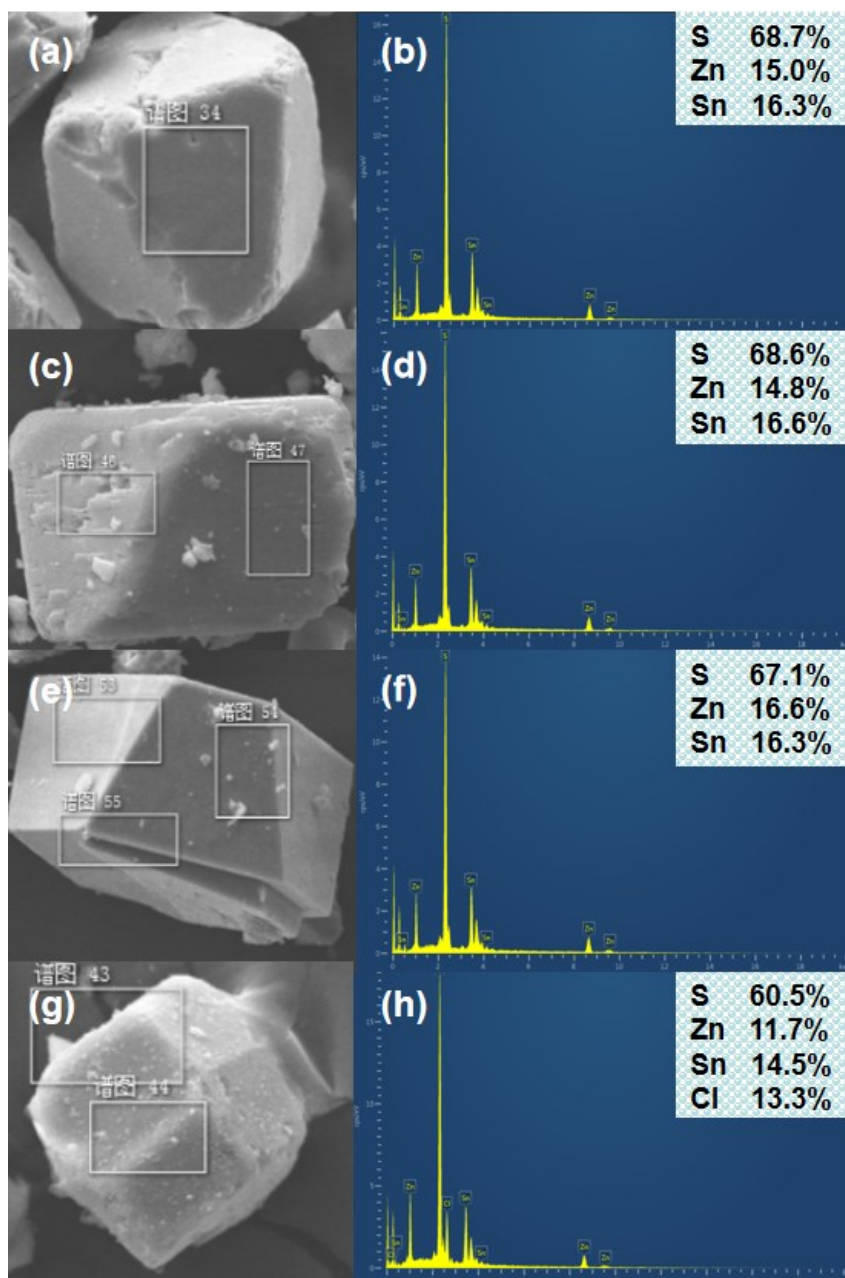


Fig. S1. SEM images (left) and EDS results (right) for **ISC-24-ZnSnS**, **ISC-25-ZnSnS-SPh**, **ISC-25-4'-NH₂**, and **ISC-26-4'-Cl**. (a-b) **ISC-24-ZnSnS**; (c-d) **ISC-25-ZnSnS-SPh**; (e-f) **ISC-25-4'-NH₂**; (d&h) **ISC-26-4'-Cl**. A large number of organic template molecules and crystalline water in the channel affected the testing of C, N, O, and other elements, and only **ISC-26-4'-Cl** containing Cl elements was analyzed. The test results (11.7:14.5:13.3) is close to the theoretical value (1:1:1), indicating that the Cl element here is not free outside the cluster (not from the residue in the raw material SnCl₂, and no Cl element was found in the test of other crystals). For all samples tested above, the ratio of Zn:Sn:S is close to 4:4:17, which is consistent with SCXRD data.

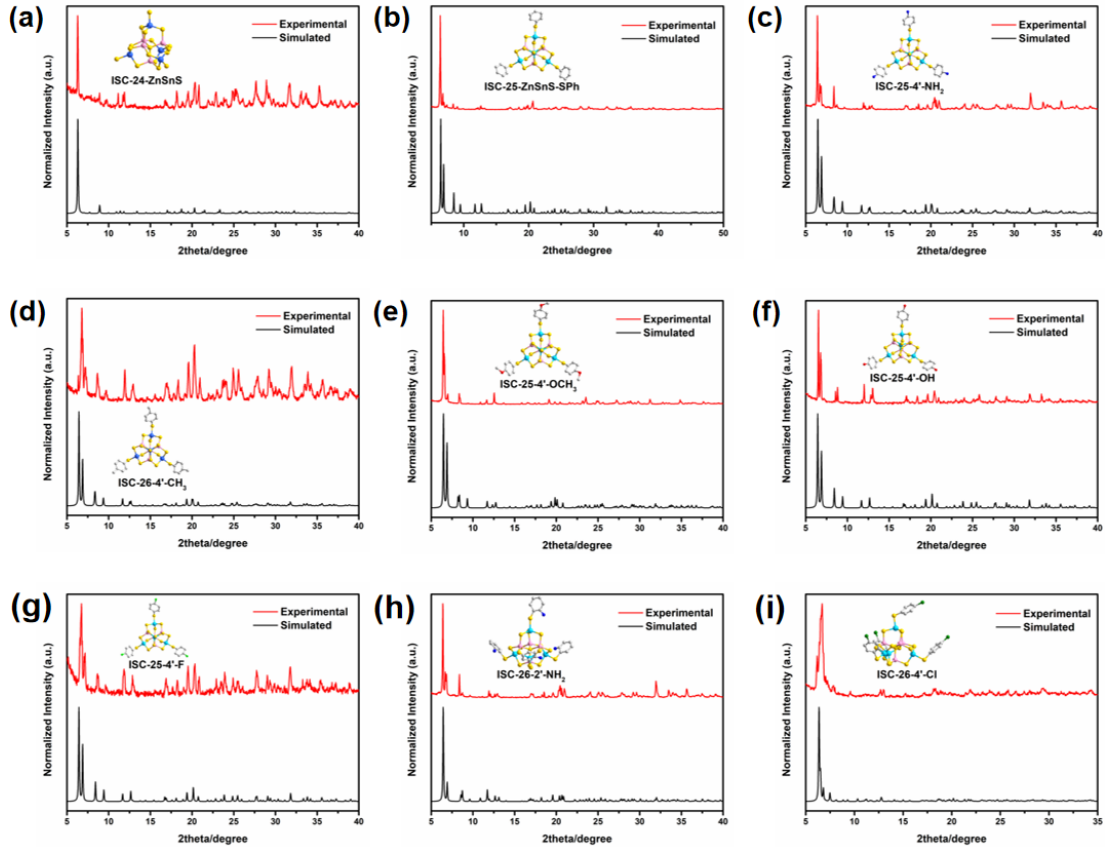


Fig. S2. PXRD results for the as-synthesized compounds of (a) **ISC-24-ZnSnS**; (b) **ISC-25-ZnSnS-SPh**; (c) **ISC-25-4'-NH₂**; (d) **ISC-25-4'-CH₃**; (e) **ISC-25-4'-OCH₃**; (f) **ISC-25-4'-OH**; (g) **ISC-25-4'-F**; (h) **ISC-26-2'-NH₂**, and (i) **ISC-25-4'-CH₃**.

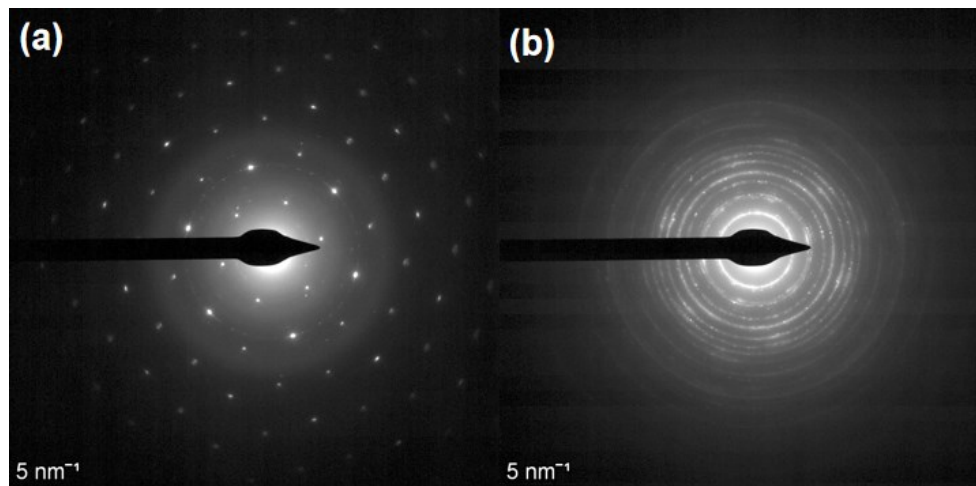


Fig. S3. SAED patterns for (a) **Ti₃C₂T_x** nanosheets and (b) **ISC-25-4'-NH₂** derived **P1-CNPs/Ti₃C₂T_x** nanocomposites.

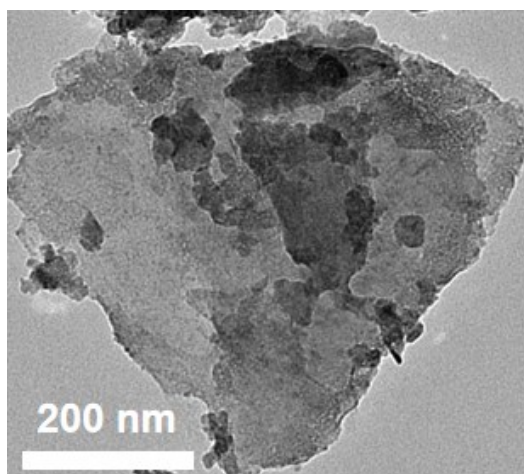


Fig. S4. TEM image of the sandwich-like structure in ISC-25-4'-NH₂ derived CM10.

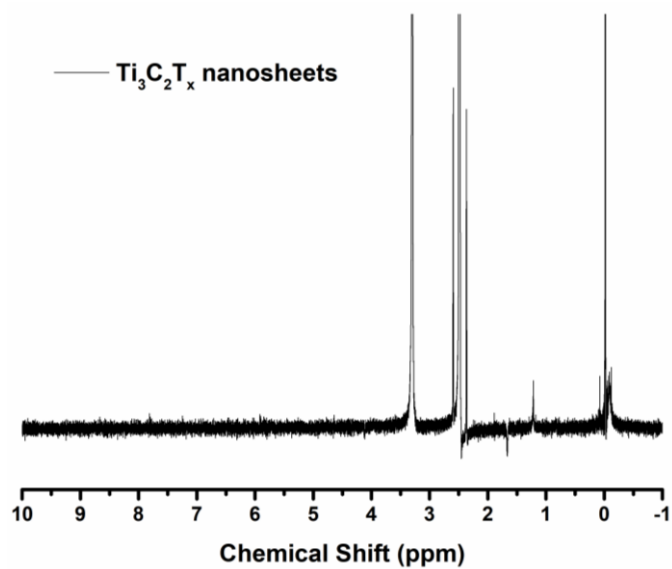


Fig. S5. ¹H-NMR spectrum of Ti₃C₂T_x nanosheets.

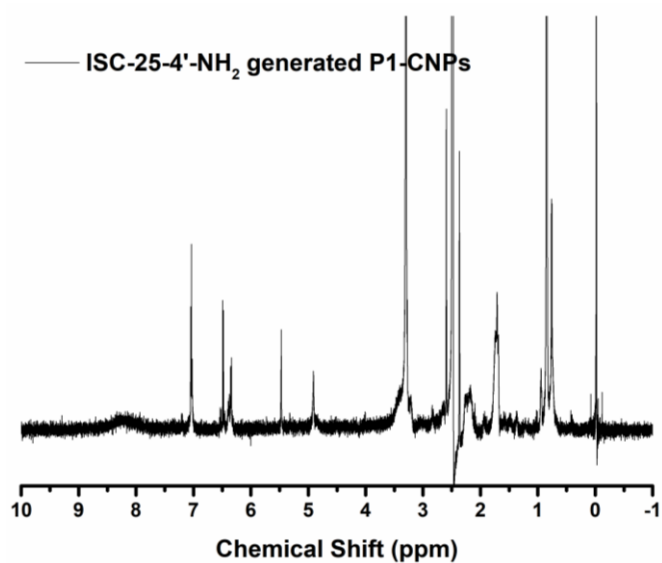


Fig. S6. ¹H-NMR spectrum of P1-CNPs formed by ISC-25-4'-NH₂.

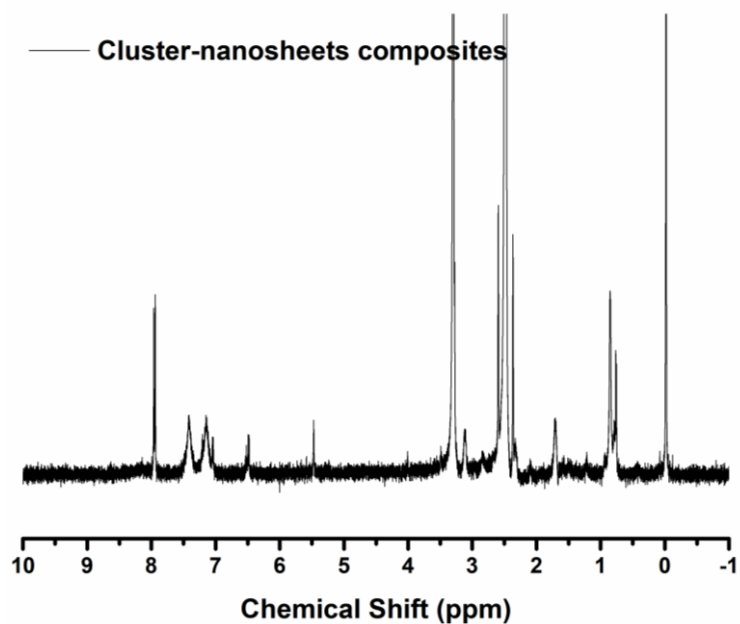


Fig. S7. $^1\text{H-NMR}$ spectrum of CM1 generated by $\text{Ti}_3\text{C}_2\text{T}_x$ nanosheets and ISC-25-4'- NH_2 derived P1-CNPs.

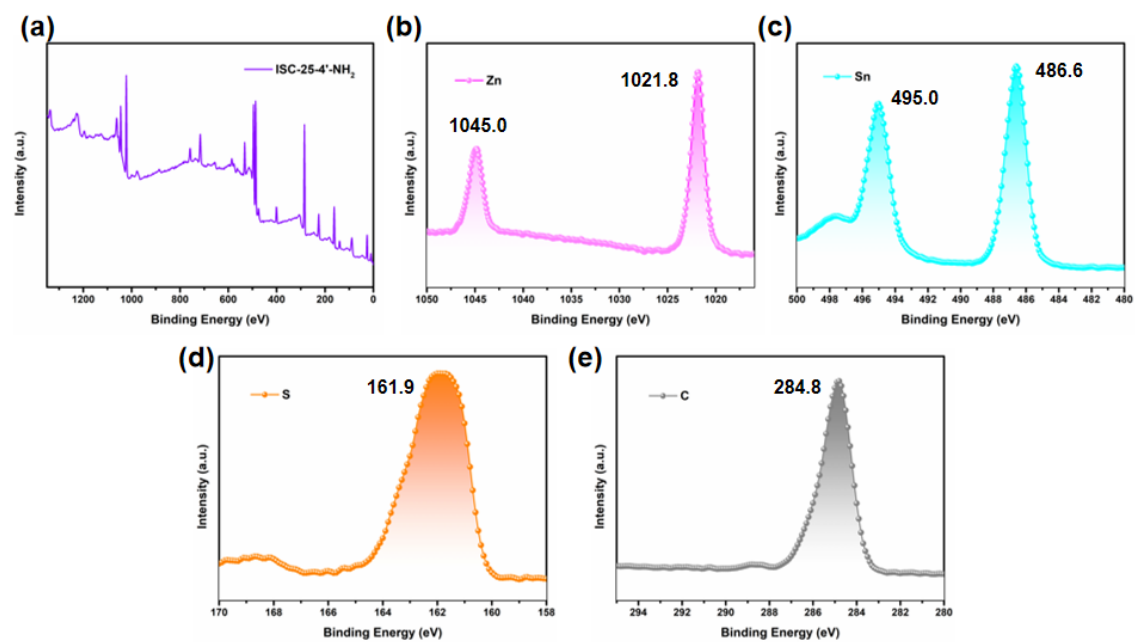


Fig. S8. XPS spectra of crystalline ISC-25-4'- NH_2 : (a) survey; (b) Zn 2p; (c) Sn 3d; (d) S 2p; (e) C 1s.

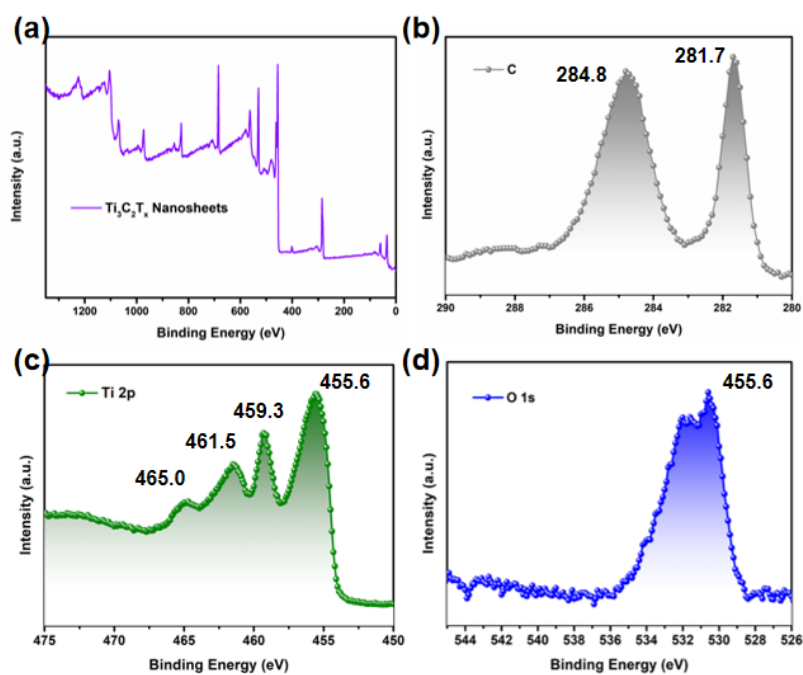


Fig. S9. XPS spectra of $\text{Ti}_3\text{C}_2\text{T}_x$ nanosheets: (a) survey; (b) C 1s; (c) Ti 2p; (d) O 1s.

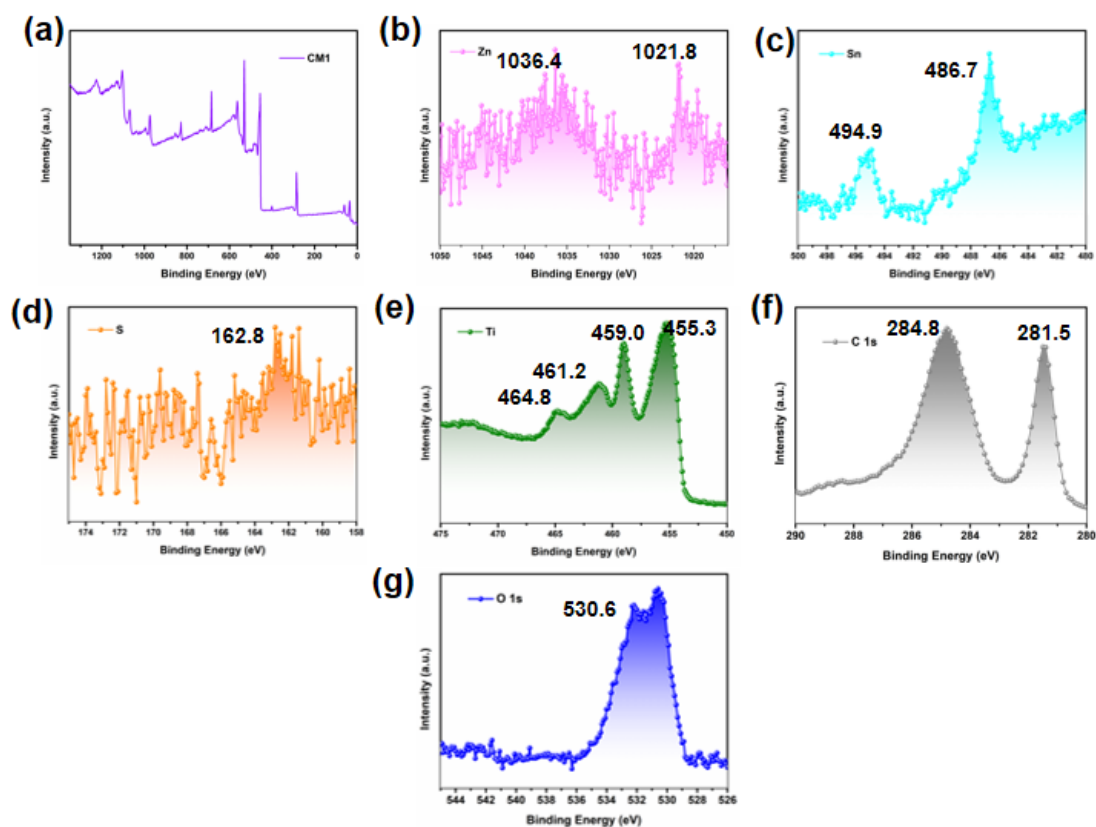


Fig. S10. XPS spectra of CM1 generated by $\text{Ti}_3\text{C}_2\text{T}_x$ nanosheets and ISC-25-4'- NH_2 derived P1-CNPs: (a) survey; (b) Zn 2p; (c) Sn 3d; (d) S 2p; (e) Ti 2p; (f) S 2p; (g) O 1s.

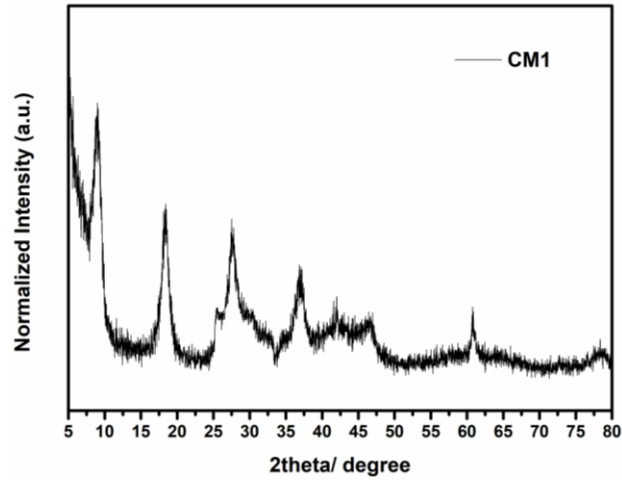


Fig. S11. PXRD result for the nanocomposites **CM1** derived from **ISC-25-4'-NH₂** and MXene nanosheets.

References:

1. L. J. Bourhis, O. V. Dolomanov, R. J. Gildea, J. A. K. Howard and H. Puschmann, *Acta Crystallogr., Sect. A: Found. Adv.*, **2015**, 71, 59-75.
2. O. V. Dolomanov, L. J. Bourhis, R. J. Gildea, J. A. K. Howard and H. Puschmann, *J. Appl. Crystallogr.*, **2009**, 42, 339-341.
3. G. M. Sheldrick, *Acta Crystallogr., Sect. C: Struct. Chem.*, **2015**, 71,3-8.
4. P. van der Sluis and A. L. Spek, *Acta Crystallogr., Sect. A: Found. Crystallogr.*, **1990**, 46, 194-201.